Cross-scale inference and wavefront reconstruction

Suman Kumar Maji, Thierry Fusco, Hussein Yahia

S. K. Maji[(a)]
T. Fusco[(b)]
H. Yahia[(a)]
[(a)] INRIA (France)
[(b)] ONERA (France)
suman-kumar.maji@inria.fr
thierry.fusco@onera.fr
hussein.yahia@inria.fr

SPIE. ASTRONOMICAL TELESCOPES + INSTRUMENTATION

Cross-scale inference and wavefront reconstruction

Introduction

A novel solution method using multiscale and **nonlinear signal processing** is proposed for the reconstruction of a turbulent phase in AO. Instead of using classical inverse problem formulations [1, 2, 3], we make use of advanced nonlinear and multiscale analysis methods in signal processing for reconstructing the wavefront phase using ideas derived from statistical physics and the framework of Microcanonical Multiscale Formalism (MMF), which is a geometric approach to multifractality. Firstly, geometrically localized singularity exponents and important parameters are computed for atmospheric turbulence. We then design a methodology, based on precise computation of the SEs [4], by which optimal inference across the scales of a turbulent phase is made possible, and we show it can be used to reconstruct a high-resolution phase from its low-resolution gradient measurements under various noise conditions. The proposed nonlinear method outperforms classical inversion techniques.

Multifractal systems in a Microcanonical Formulation (MMF)

$\mathfrak{E}_{\mathbf{l}}(\mathbf{x})$: scale-dependent functional. Signal s is multifractal in a microcanonical sense [5]: for at least one functional $\mathfrak{E}_{\mathbf{l}}(\mathbf{x})$:

$$\mathfrak{E}_{\mathbf{l}}(\mathbf{x}) = \alpha(\mathbf{x})\mathbf{l}^{h(\mathbf{x})} + o(\mathbf{l}^{h(\mathbf{x})}) \quad (\mathbf{l} \to 0) \tag{1}$$

Exponent $h(\mathbf{x})$: *singularity exponent* at point $\mathbf{x}$. In practical application:

$$\mathfrak{E}_{\mathbf{l}}(\mathbf{x}) = \int_{\mathcal{B}(\mathbf{x},\mathbf{l})} \|\nabla \mathbf{s}\|(\mathbf{y})\mathbf{d}(\mathbf{y}) \tag{2}$$

Figure 1. From left to right: True phase used for experimental purpose (size 128×128 pixels), psf associated with the true phase, SE's computed over the true phase (using equation (5)), reconstructed phase using the SE's.

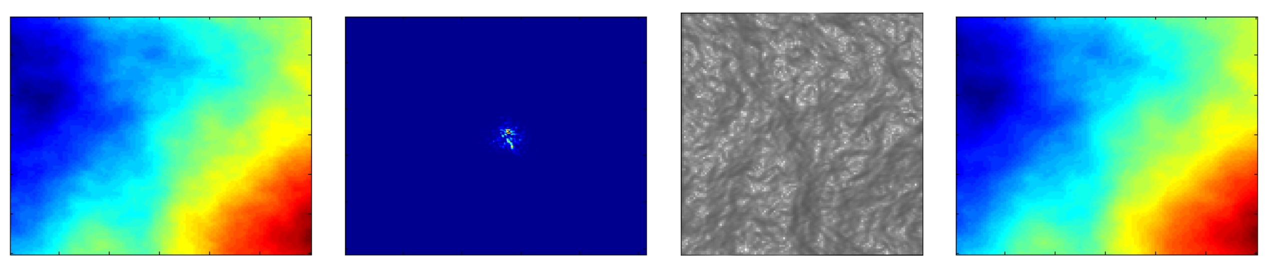

Singularity analysis

Multifractal hierarchy:

$$\mathcal{F}_h = \{\mathbf{x} : h(\mathbf{x}) = h\} \tag{3}$$

Let $\mathcal{T}_\Psi(\mathfrak{E}_{\mathbf{l}}(\mathbf{x}))$ be the wavelet projection of $\mathfrak{E}_{\mathbf{l}}(\mathbf{x})$ with mother wavelet Ψ:

$$\mathcal{T}_\Psi(\mathfrak{E}_{\mathbf{l}}(\mathbf{x})) = \frac{1}{\mathbf{l}^2}\int_{\mathbb{R}^2} \|\nabla \mathbf{s}\|(\mathbf{y})\Psi(\frac{\mathbf{x}-\mathbf{y}}{\mathbf{l}})\mathbf{d}(\mathbf{y}) \; . \tag{4}$$

Then:

$$h(\mathbf{x}) = \frac{\log(\mathcal{T}_\Psi(\mathfrak{E}_{\mathbf{l}}(\mathbf{x}))/\langle\mathcal{T}_\Psi(\mathfrak{E}_{\mathbf{l}}(\cdot))\rangle)}{\log \mathbf{l}} + o\left(\frac{1}{\log \mathbf{l}}\right) \tag{5}$$

Results

Reconstruction has been done for 1000 phase-screens provided by ONERA, with gradients of three different sizes (16×16 pixels, 32×32 pixels and 64×64 pixels respectively). We then calculate the residual phase for all the 1000 reconstructed phases and compute the average power spectral density (PSD) of the residual phases. We then plot the PSD against spatial frequency and compare our results with the LS estimator. The results clearly show the superiority of our algorithm, with the classical LS estimator, under different levels of SNR (the residual phase error being less in our case). We repeat the same operation with cases where we take the SE's computed over an average instance of the true phase and a fixed FFT based Kolmogorov phase. We can see on figures that the overall performance of the reconstruction using our technique is much better than the LS estimator, especially in the case of very low-level SNR's.

Figure 2. Results of the reconstruction in a noisy environment. **Top row :** Reconstructed phase under different levels of SNR. **Bottom row :** Comparison of the PSD between the true phase and the reconstructed phase under different levels of SNR.

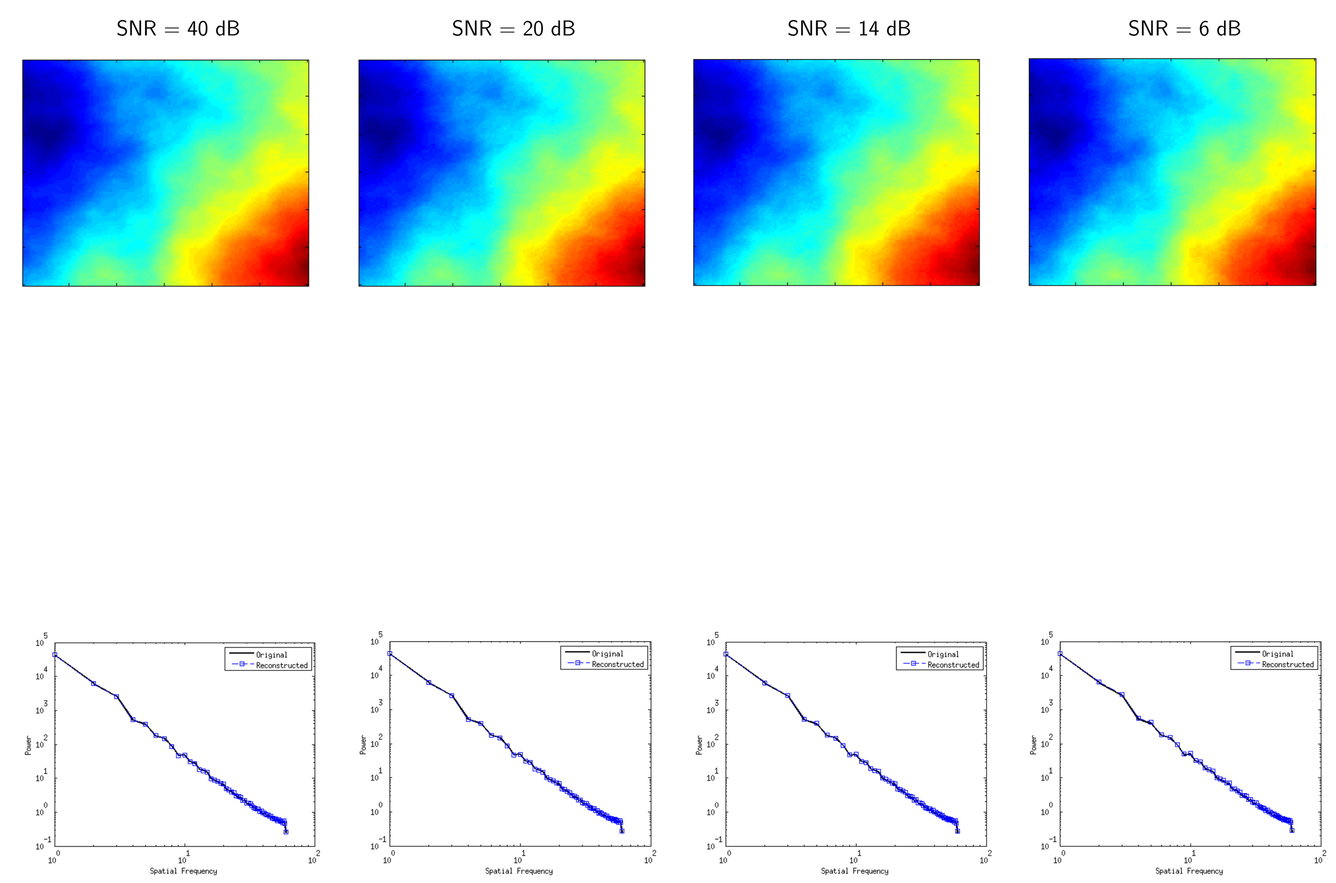

Figure 3. Performance under noise - Point spread function (psf). The y-axis corresponds to the square of the normalized image plane irradience and the x-axis corresponds to the angular distance in arseconds. **Top row :** The X cut of the psf. **Bottom row :** The Y cut of the psf. Same noise conditions as in Figure 2.

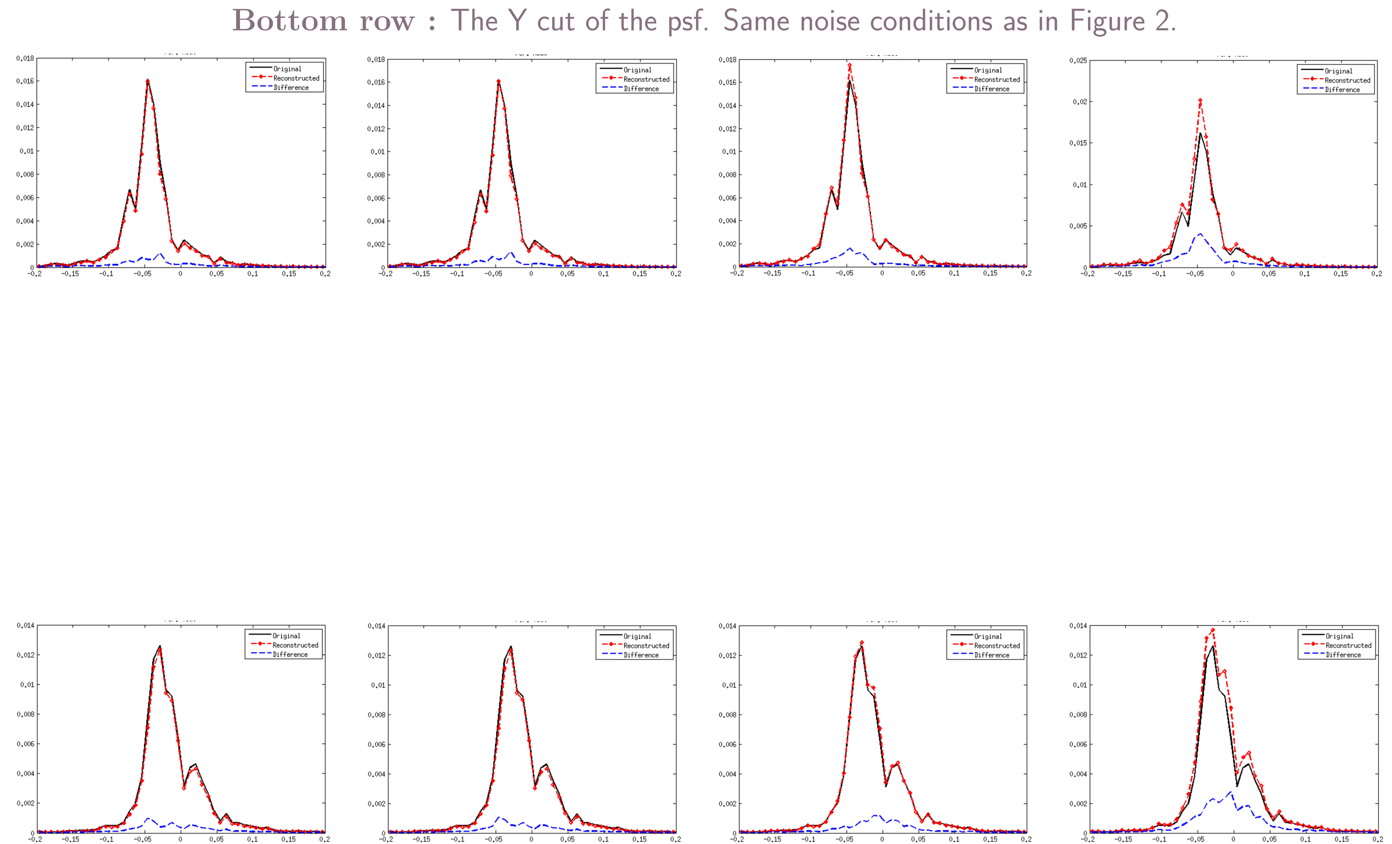

Figure 4. Comparison of the residual phase statistics with classical operators under level of SNR: 6dB. To estimate ϕ_{cor} using the MMF technique, we use the singularity exponents computed over the average phase instance (obtained by averaging the 10 previous and 10 post instances of the true phase) as input high-resolution phase in the decomposition process of our algorithm.

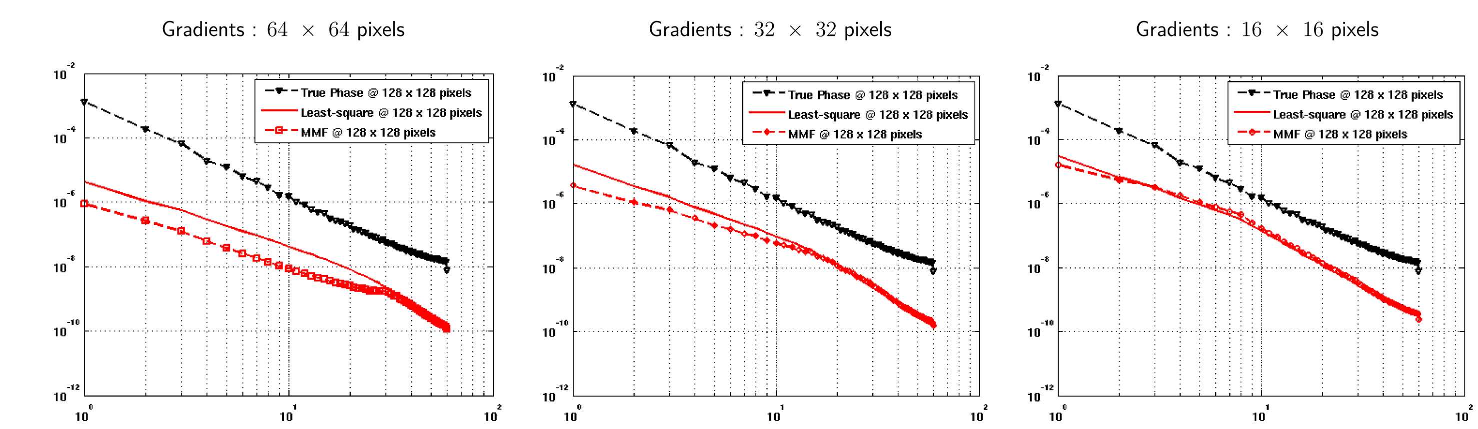

Figure 5. Comparison of the residual phase statistics with classical operators under level of SNR: 6dB. To estimate ϕ_{cor} using the MMF technique, we use the singularity exponents computed over a fixed FFT based Kolmogorov phase screen as input high-resolution phase in the decomposition process of our algorithm.

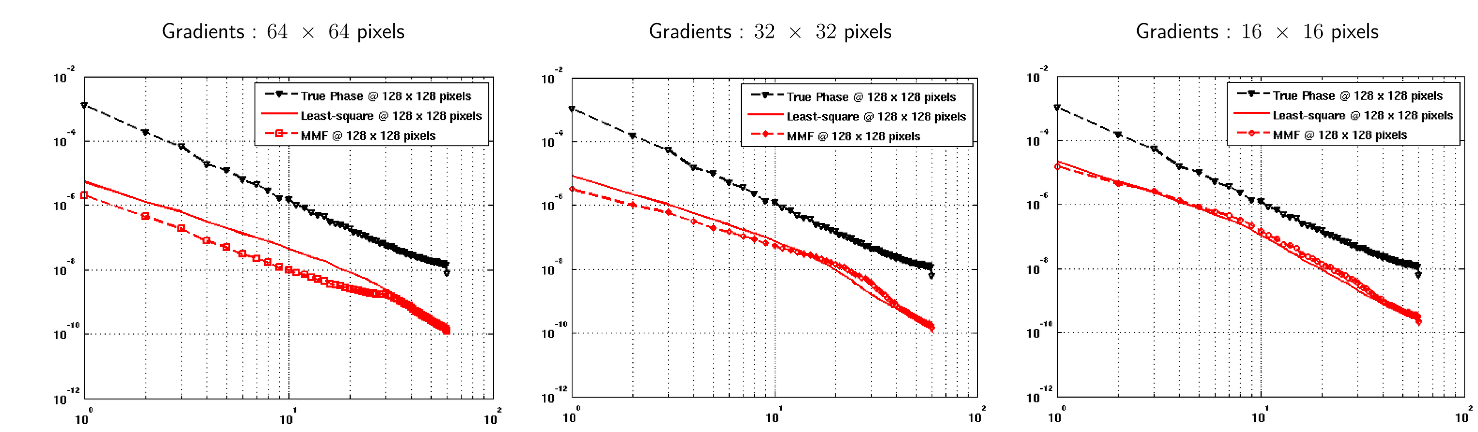

Acknowledgment and references

Suman Kumar Maji's PhD is funded by a CORDIS grant and Région Aquitaine OPTAD research project grant.

References

[1] Bardsley, J. M., "Wavefront reconstruction methods for adaptive optics systems on ground-based telescopes," *SIAM J. Matrix Analysis Applications* **30**, 67–83 (2008).

[2] Mugnier, L., Besnerais, G. L., and Meimon, S., [*Inversion in optical imaging through atmospheric turbulence in Bayesian approach to inverse problems*], Jérôme Idier ed., ISTE, John Wiley & Sons Inc. (2008). ISBN: 878-1-84821-032-5.

[3] Gilles, L., Vogel, C. R., and Ellerbroek, B. L., "A multigrid preconditioned conjugate gradient method for large scale wavefront reconstruction," *J. Opt. Soc. Am. A* **19**, 1817–1822 (2002).

[4] Turiel, A., Pérez-Vicente, C. J., and Grazzini, J., "Numerical methods for the estimation of multifractal singularity spectra on sampled data: A comparative study," *Journal of Computational Physics* **216**, 362–390 (2006).

[5] Maji, S. K. and Yahia, H., "Edges, transitions and criticality," *Pattern Recognition, Elsevier* **47**, 2104–2115 (2014).

Inria INVENTEURS DU MONDE NUMÉRIQUE
ONERA THE FRENCH AEROSPACE LAB